SUPPLEMENTARY INFORMATION FOR

The Endonuclease APE1 Processes miR-92b Formation, Thereby Regulating Expression of the Tumor Suppressor LDLR in Cervical Cancer Cells

SUPPLEMENTARY FIGURES

Supplementary Fig. 1. miR-to-pri-miR ratios quantified in CH12F3 cells with APE1 KO. (a) Western blotting validation of $APE1^{-/-}$ knockout (KO) in CH12F3 cells. (b) Total RNA was purified from CH12F3 cells, either $APE1^{+/+}$ or $APE1^{-/-}$ KO, and cDNA was prepared by reverse transcription. Mature miR-92b levels were normalized to RNU44, while pri-miR-92b levels were normalized to GAPDH. Data are represented as means ± SEMs. *P<0.05, **P<0.01.

Supplementary Fig. 2. APE1 inhibitors decrease APE1's abasic site incision activity. (a) HeLa cells incubated with fiduxosin (FDX, 40 µM), compound #3 (20 µM), or E3330 (100 µM) for 24 h or HeLa cells with siRNA-mediated APE1 KD were used to prepare cell extracts whose APE1 endonuclease action was quantified in vitro. Histogram representation of the kinetics of endonuclease activity in cell extract (12.5 ng) denoted as transformation of a substrate (S) containing an abasic site to the incised product (P) expressed as a percentage. Typical image of a polyacrylamide gel under denaturing conditions of the enzymatic reactions. (b) APE1 protein levels in HeLa cells incubated with fiduxosin (FDX, 40 µM), compound #3 (20 µM), or E3330 (100 µM) for 24 h or HeLa cells with siRNA-mediated APE1 KD. Typical Western blots of total HeLa cell extracts using an anti-APE1 antibody with tubulin normalization. NE = no cell extract, NT = non-treated cells. Data are represented as means ± SEMs. *P<0.05, **P<0.01.

Supplementary Fig. 3. Oxidative stress induces an interaction between APE1 and DROSHA.

(a) The Duolink proximity ligation assay (PLA) was performed with antibodies against APE1 and DROSHA to quantify the interaction between APE1 and DROSHA within the nucleoplasm following oxidative stress. HeLa cells were incubated with hydrogen peroxide (H_2O_2, 1 mM) for a duration of 15, 30, and 60 minutes on coverslips. APE1-FITC was selected as the fluorescent staining reference for cell nuclei. (b) The chart

represents Duolink PLA signals per cell in a minimum of 30 cells chosen at random per experimental condition. (c, d) HeLa cells were exposed to H_2O_2 (1 mM) for 15 minutes and then rested for 1, 3, or 6 hours post H_2O_2-treatment and had their levels of mature miR-92b and miR-92b quantified by qRT-PCR. Mature miR and pri-miR levels were normalized to RNU44 and GAPDH, respectively. NT = non-treated. (e) HeLa cells with APE1 KD had their total RNA purified and reacted to a probe with an aldehyde-reactive group (ARP), which targets oxidatively-damaged AP sites. ARP-bound RNA was precipitated using magnetic beads and underwent qRT-PCR with TaqMan probes for pri-miR-92b or miR-92b. Differences in oxidative damage to miRs were assessed according to variation in Ct values for oxidized versus total RNA. Data are represented as means ± SEMs. *P<0.05, **P<0.01.

Supplementary Fig. 4. miR-92b directly suppresses LDLR expression in human cervical carcinoma cells. (a) The human LDLR gene displays two putative binding sites for miR-92b. (b) SiHa and (c) CaSki cells with transient transfection of miR-92b mimics had lowered LDLR protein levels as measured by WB (top panels) and were semi-quantified by densitometry analysis (bottom panels). (d) HEK 293T cells were infected with pMIR-REPORT-WT-3'-UTR-LDLR (WT 3'-UTR) or pMIR-REPORT-mutant-3'-UTR-LDLR (mutant 3'-UTR), which were co-transfected with either hsa-miR-92b mimics or a scrambled negative control (NC). A Renilla luciferase plasmid was co-transfected to serve as an internal standard and relative luminescence signals were calculated. (e) Inverse relationship between miR-92b and LDLR levels in human tumor biopsy samples by Spearman correlation analysis (R^2 = 0.2972, P<0.01). Data are represented as means ± SEMs. *P<0.05, **P<0.01.

Supplementary Fig. 5. miR-92b upregulated in human cervical cancer tumors

qRT-PCR analysis of (a) APE1 mRNA, (b) miR-92b, and (c) LDLR mRNA levels in human cervical cancer biopsy samples (n=50) and matching healthy cervical tissue (n=50). miR-92b displays significantly higher expression in tumor biopsies relative to matching healthy cervical tissue.

Supplementary Fig. 6. Validation of siRNA-mediated LDLR knockdown in human cervical carcinoma cells. Western blotting analysis revealed that si-LDLR-1 and si-LDLR-2 siRNAs profoundly reduce LDLR protein expression in CaSki and SiHa cells.

Supplementary Fig. 1

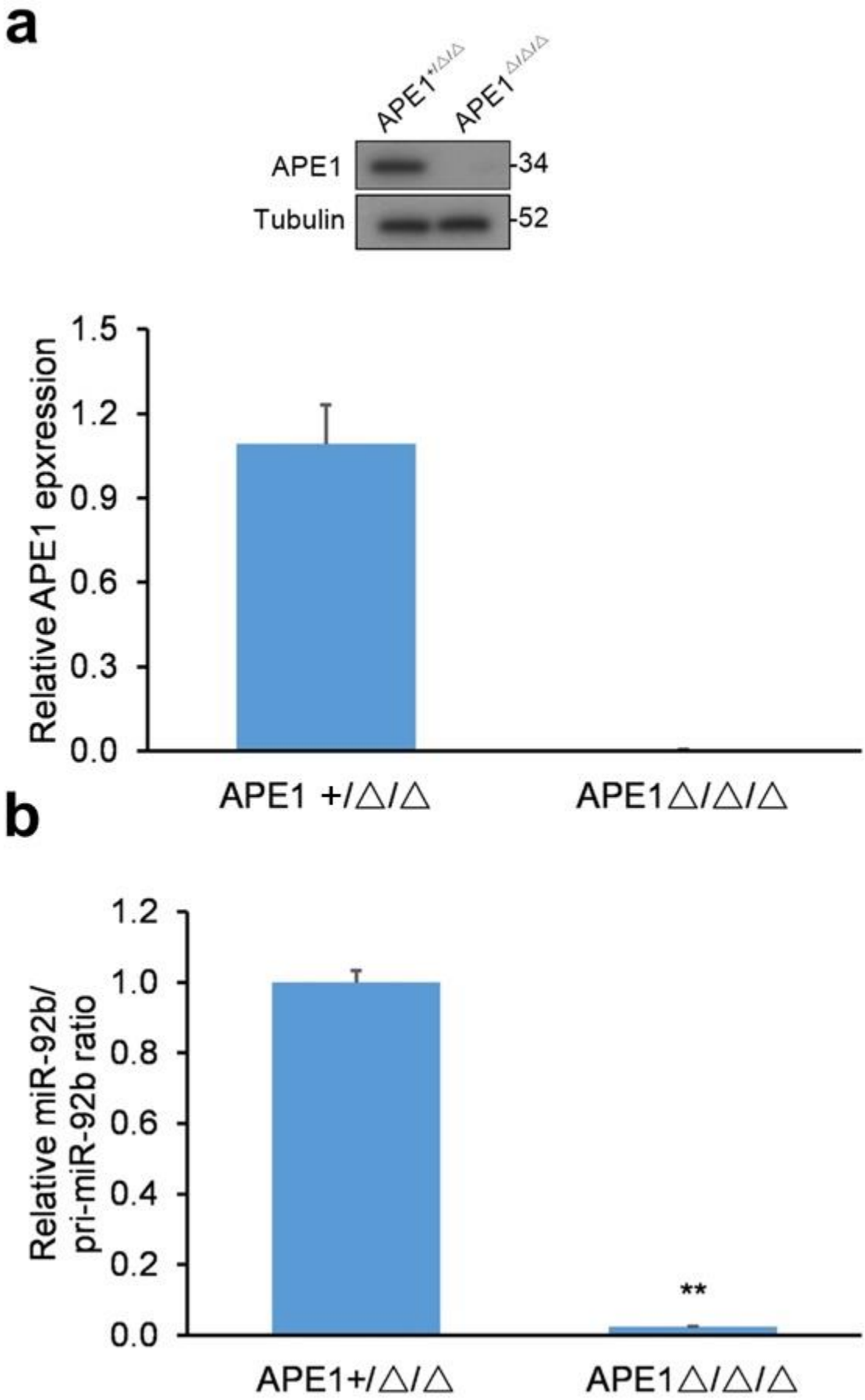

Supplementary Fig. 2

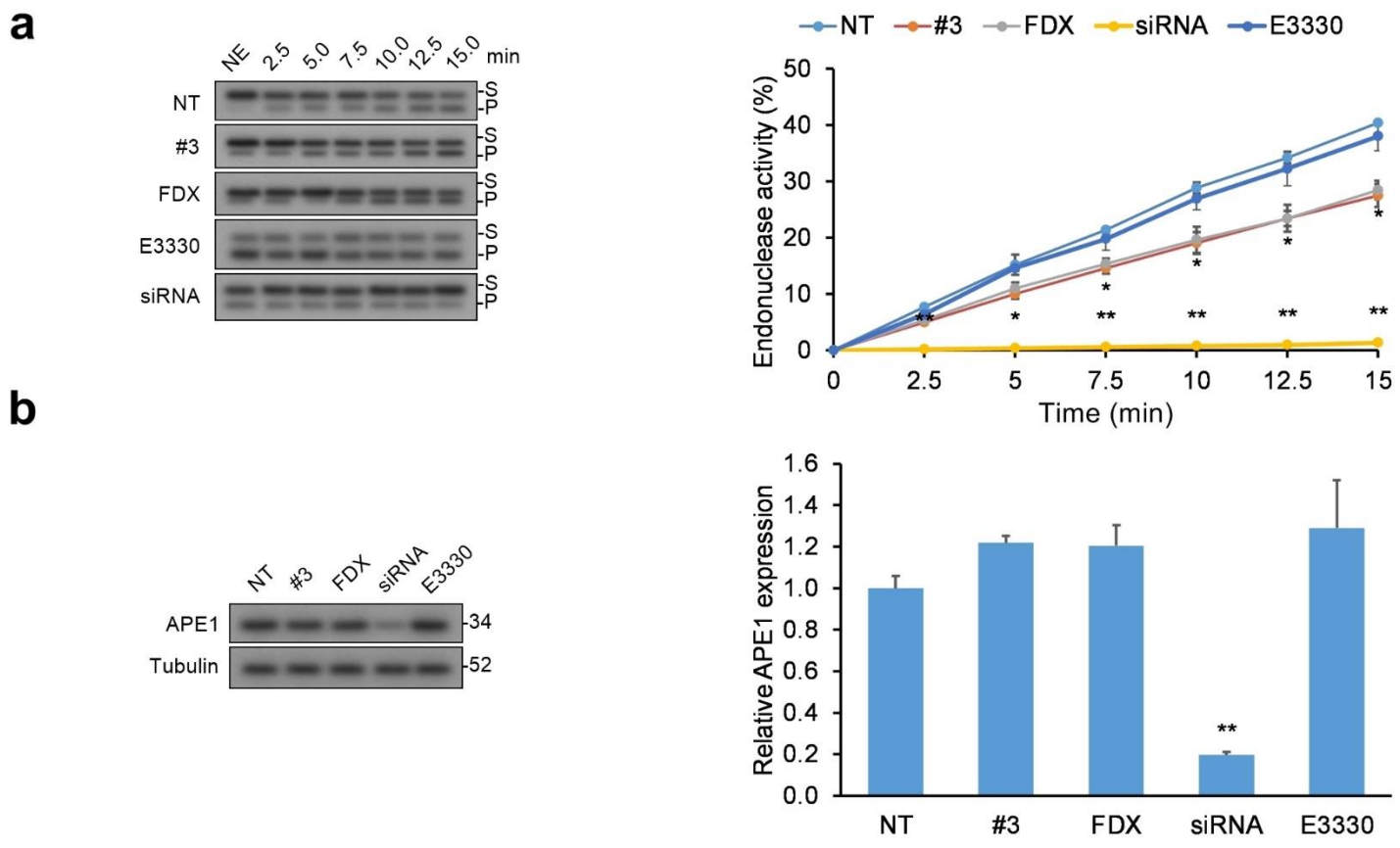

Supplementary Fig. 3

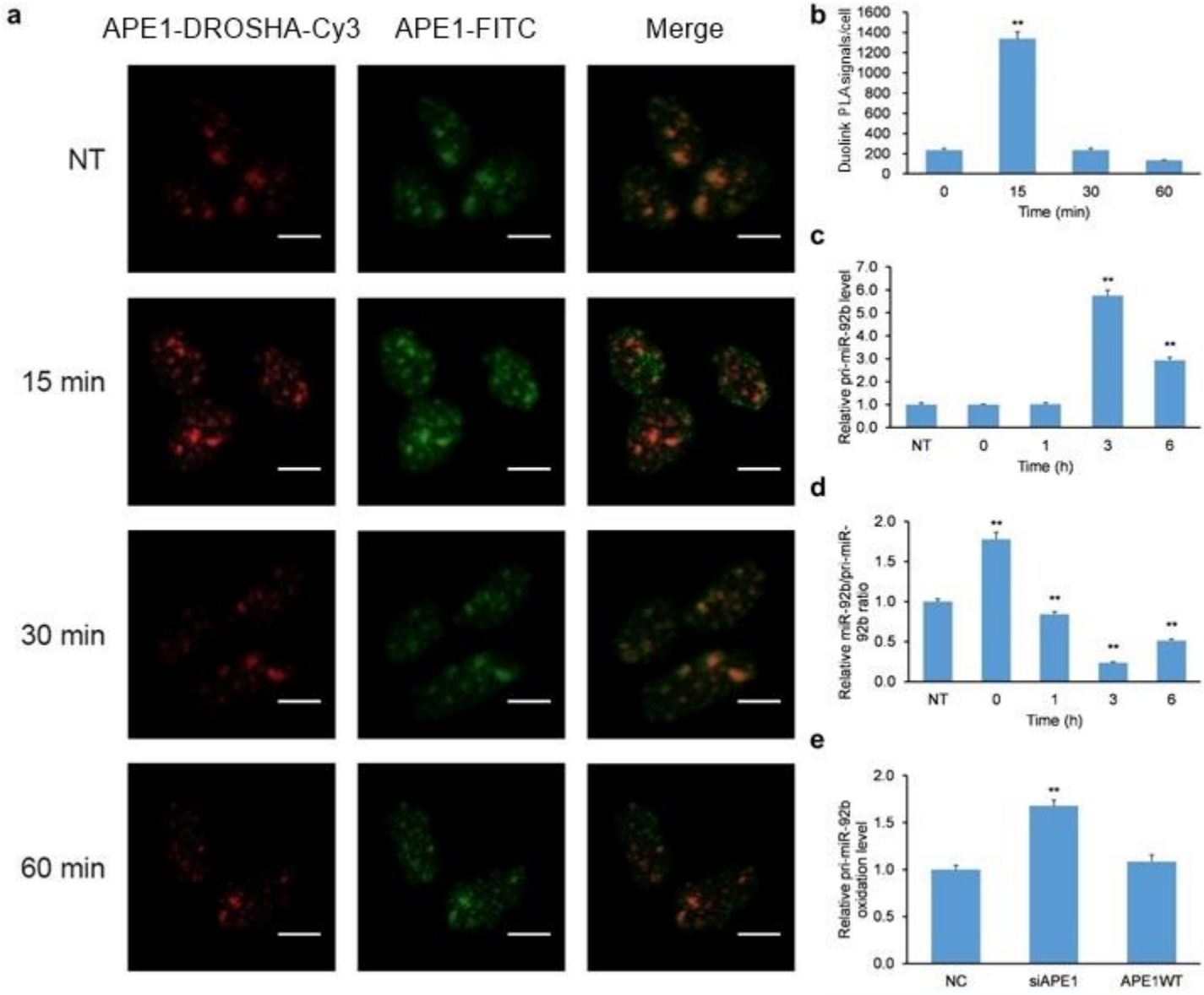

Supplementary Fig. 4

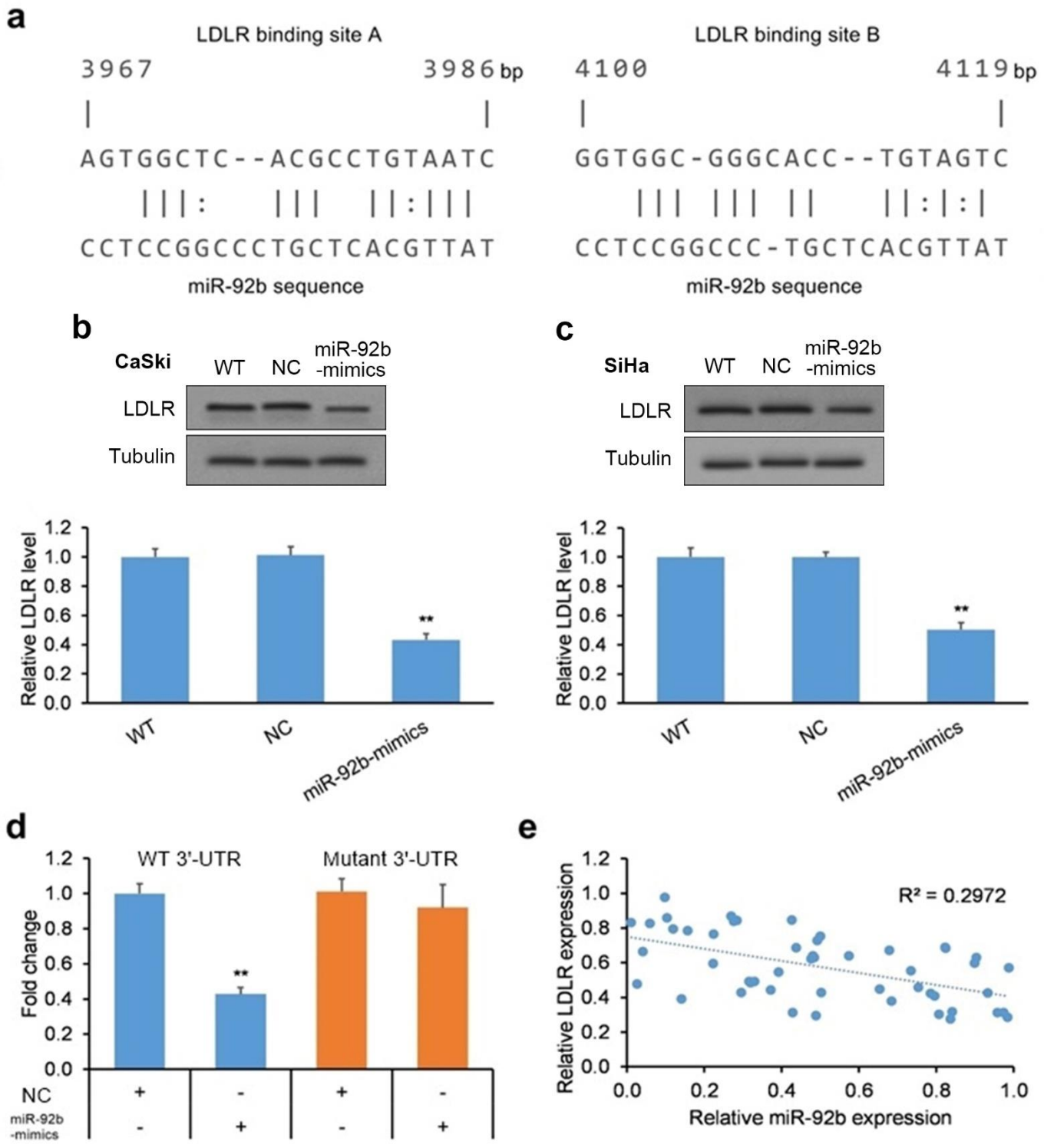

Supplementary Fig. 5

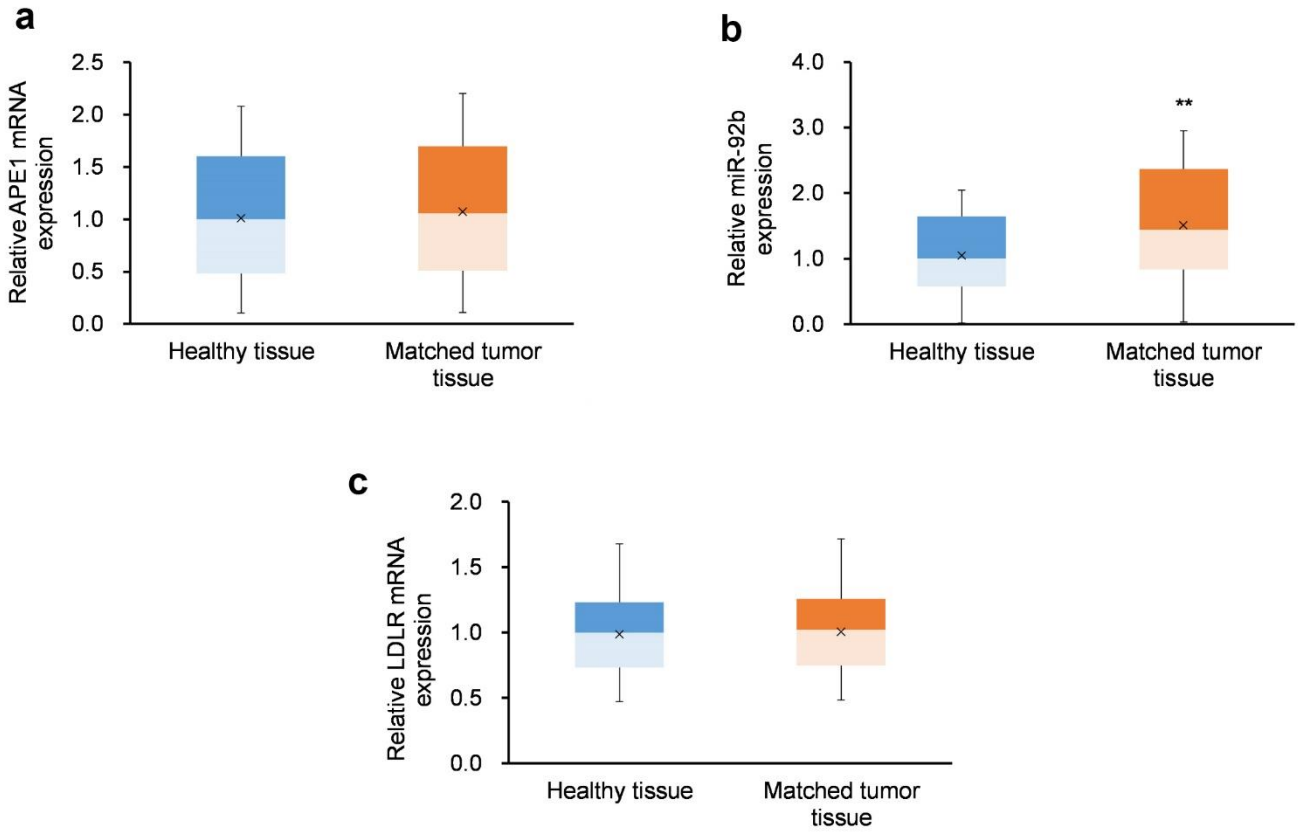

Supplementary Fig. 6